mixtures involving CD_2Cl_2 (Table s-II), values of $\Delta H^{\ddagger}$, $\Delta S^{\ddagger}$, C_M, E_M, C_O, E_O, and C_ω recalculated for proton line-broadening data of $Mn(ClO_4)_2$ (Table s-III), values of S, τ_{e2}, τ_{c2}, C_{DD}, A, and C_{HF} (Table s-IV), temperature dependence of the line widths for oxygen-17 of HOAc in the absence of metal ions (Figure s-1), and temperature dependence of proton line broadening for $Cu(ClO_4)_2$ in a mixture of acetic acid with CD_2Cl_2 (Figure s-2) (9 pages). Ordering information is given on any current masthead page.

Contribution from the Institutes of Inorganic Chemistry, University of Zurich, 8057 Zurich, Switzerland, and Technical University of Aachen, D-5100 Aachen, West Germany

EPR Studies of the Electronic Structure and Dynamic Jahn-Teller Effect in Cobalt(II) Mixed-Sandwich Compounds

B. L. Ramakrishna,*[1a,b] A. K. Salzer,[1b] U. Ruppli,[1b] J. H. Ammeter,[1b] and U. Kölle[1c]

Received July 12, 1985

EPR studies are reported on the 19-electron sandwich complex $Co(cp)(Bz)^+$ ($(\eta^5\text{-}C_5H_5)Co(\eta^6\text{-}C_6H_6)^+$) and some of its ring-methylated derivatives in several diamagnetic host lattices and frozen solutions. The results are consistent with a d^7 configuration for cobalt with the unpaired electron in the e_{1g} orbital having largely metal (d_{xz},d_{yz}) character. The dependence of the EPR parameters on the host lattice is mainly attributed to the rhombic splitting caused by the unsymmetrical host lattice potential acting on the dynamically Jahn-Teller-coupled $^2\pi$ ground state. The bonding parameters have been compared with those of analogous compounds with the covalency decreasing as $Ni(cp)_2^+ > Co(Pmcp)(hmBz)^+ > Co(cp)(Bz)^+ > Co(cp)_2^+ > Fe(cp)(Bz)$. The variation of line width with temperature has been used to derive information on the energy of the first excited Kramers doublet.

Introduction

Electron paramagnetic resonance of sandwich compounds with degenerate or nearly degenerate electronic ground states yields information on the bonding parameters on the one hand and the dynamic Jahn-Teller effect on the other.[2] The systems studied are mostly d^5 and d^7 sandwich compounds of the first-row transition-metal series. The main phenomenon observed in all the above cases is a dependence of the EPR parameters—**g** and **A** tensors—on the host lattice, attributable mainly to the changes in the relative composition of the ground electronic state wave function caused by the changes in the low-symmetry components of the solvent fields and, to a lesser degree, by variations in the amplitudes of the dynamic Jahn-Teller distortions.[3]

We present in this paper the results of the investigation of a series of cobalt(II) mixed-sandwich compounds, $Co(C_5R_5)(C_6R'_6)^+$ with R and R' being CH_3 or H. Also included are the results for the bis(hexamethylbenzene)cobalt(II) dication, $Co(C_6Me_6)_2^{2+}$ (see Figure 1).[1d] A detailed report on the preparative, electrochemical, and NMR investigation on some of the complexes studied here has been presented earlier,[4] and preliminary results of the EPR studies on some of the complexes are also mentioned. In this earlier work only alkylated derivatives could be synthesized and studied by EPR, and these invariably suffer from large orthorhombic distortions (crystal field splitting $\delta >$ spin-orbit coupling ζ). It has now been possible to investigate the unsubstituted species $Co(cp)(Bz)^+$,[1d] which is expected to be the least distorted in a variety of hosts, and to derive useful information about the dynamic Jahn-Teller parameters. We have also studied $Co(Pmcp)(Bz)^+$ and $Co(cp)(hmBz)^+$ wherein the effect of methylation can be analyzed, and further we have provided the data on $Co(Pmcp)(hmBz)^+$ wherein both the rings are fully methylated. For the sake of comparison, we have included the results on $Co(hmBz)_2^{2+}$.

The motivation of this study is to investigate (1) the mixed sandwich effect, (2) the effect of methylation, (3) a comparison of the effect, especially of covalency parameters, with that for other d^7 sandwiches including cobaltocene and its methylated derivatives, Fe(I) sandwich compounds, and Ni(III) sandwich compounds, (4) the degree of orthorhombic distortion in various host lattices, and (5) the relaxation behavior, through line width studies.

Whereas large δ values (obtainable through methylation) are required for narrow EPR line widths, accessibility of spectra up to high temperatures, and for the close approach to the static limit, low values of δ (unmethylated compound) are required for significant dynamic effects so that the whole range of $V = 0$–1 (i.e. dynamic to static Jahn-Teller cases) can be investigated.

Experimental Section

Synthesis. Preparation and handling of all the complexes and solvents were carried out under a purified N_2 atmosphere with Schlenk-type apparatus.

The diamagnetic air-stable dications were reduced in solution with cobaltocene to the paramagnetic monocations, which were stable only under rigorous exclusion of air below −30 °C. A side product is the diamagnetic cobaltocenium cation. From this resulting salt mixture the cobaltocene salt was separated by fractional crystallization from methylene chloride/toluene, where it is much less soluble than the monocation mixed-sandwich salts. These monocations were directly measured in solution, or a large excess of the matrix salt was added until a saturated solution was obtained and a diamagnetically diluted microcrystalline precipitate was obtained on adding pentane. This was then filtered, dried under vacuum, and transferred to EPR tubes and sealed under a He atmosphere.

EPR Measurements. EPR spectra were recorded on a Varian E-line spectrometer operating at X-band frequency. The magnetic field was calibrated by using a Varian NMR gaussmeter, and the microwave frequency was measured by using a EIP frequency counter. Temperature control was achieved by using an Oxford Instruments ESR-9 liquid-helium cryostat of the continuous flow type, and temperature measurements were made by using a thermocouple situated just below the sample tube. Quartz EPR sample tubes were charged in a nitrogen-filled glovebox and sealed under 500 mbar of He gas in order to improve heat exchange. The EPR spectra were simulated by using a powder simulation program.[5]

Theoretical Background

As in metallocenes, the d-orbital splitting in bis(arene) and mixed-sandwich compounds can be described by a pseudoaxial symmetry[6] even though the exact molecular point groups are D_{6h} and C_s, respectively.[7] Thus, analogous to that of $Co(cp)_2$, the ground state is expected to be $^2E_{1g}$ (in the D_{6h} notation) or $^2\pi$ (in the $C_{\infty v}$ notation), with the unpaired electron in the e_{1g} orbital having the metal (d_{xz},d_{yz}) character.

(1) (a) Present address: Department of Chemistry, Arizona State University, Tempe, AZ 85287. (b) University of Zurich. (c) Technical University of Aachen. (d) In this paper, the abbreviation Bz is used in a nonstandard manner.
(2) (a) Ammeter, J. H. *J. Magn. Reson.* **1978**, *30*, 229 and references therein. (b) Clack, D. W.; Warren, K. D. *Struct. Bonding (Berlin)* **1980**, 39, 1 and references therein.
(3) Ammeter, J. H.; Zoller, L.; Bachmann, J.; Baltzer, P.; Gamp, E.; Deiss, E. *Helv. Chim. Acta* **1981**, *64*, 1063.
(4) Kölle, U.; Fuss, B.; Rajasekharan, M. V.; Ramakrishna, B. L.; Ammeter, J. H. Böhm, M. C., submitted for publication.
(5) Daul, C.; Schläpfer, C. W.; Mohos, B.; Ammeter, J. H. Gamp, E. *Comput. Phys. Commun.* **1981**, *21*, 385.
(6) Warren, K. D. *Struct. Bonding (Berlin)* **1976**, *27*, 45.
(7) Our semiempirical molecular orbital calculations indicate that the low-symmetry splittings in the doubly degenerate orbitals of $Co(cp)(Bz)^+$ and its methylated derivatives are negligible.

0020-1669/86/1325-1364$01.50/0

Chart I

	vibronic coupling case	static limit (first order in ζ)	
g_z	$g_e - 2k_\parallel V(\cos\alpha)$	$g_e - k_\parallel\zeta/\delta$	(1a)
$g_\perp = (g_x + g_y)/2$	$(g_e + 5x_i)(\sin\alpha)$	$g_e + 5x_i$	(1b)
$\delta(g) = g_y - g_x$	$6(1 + V(\cos\alpha))x_i$	$6x_i$	(1c)
A_z	$C_\pi^2P\{^2/_7 - \kappa - 2V(\cos\alpha) - {}^3/_7(1 - 3V(\cos\alpha))x'_i\}$	$C_\pi^2P(^2/_7 - \kappa - {}^3/_7x'_i)$	(2a)
$A_\perp = A_x + A_y)/2$	$C_\pi^2P(-{}^1/_7 - \kappa + {}^{73}/_{14}x'_i)(\sin\alpha)$	$C_\pi^2P(-{}^1/_7 - \kappa + {}^{73}/_{14}x'_i)$	(2b)
$\delta(A) = A_y - A_x$	$C_\pi^2P(-{}^6/_7 + {}^{45}/_7x'_i)(1 + V(\cos\alpha))$	$C_\pi^2P(-{}^6/_7 + {}^{45}/_7x'_i)$	(2c)

Table I. EPR Parameters of Co(II) Sandwich Compounds

no.	compd	matrix	g_x	g_y	g_z	$\Delta(g_z)$	$g_\perp$	A_x	A_y	A_z	$A_\perp$	$\delta(A)$
1	$Co(cp)(Bz)^+$	$Co(cp)_2BF_4$										
		site 1	2.008	2.067	1.815	0.187	2.038	20	140	64	80	120
		site 2	1.997	2.056	1.801	0.201	2.027	18	138.5	66	78.2	120.5
		site 3	1.979	2.038	1.795	0.207	2.008	18	137.5	69	77.8	119.5
		$Co(cp)_2PF_6$										
		site 1	1.956	2.015	1.790	0.212	1.985	18	136	72	77	118
		site 2	1.951	2.010	1.760	0.242	1.980	18	134	80	76	116
		$Fe(cp)(Bz)PF_6$	1.993	2.053	1.800	0.202	2.023	18	138	67	78	120
		acetic anhydride	2.000	2.059	1.806	0.196	2.030	18	139	65	78.5	119
		methylene chloride	2.002	2.062	1.809	0.193	2.032	19	140	64	79.5	121
2	$Co(cp)(hmBz)^+$	$Fe(cp)(hmBz)PF_6$	2.023	2.093	1.865	0.137	2.058	23	141	63	82	118
		acetic anhydride	2.020	2.090	1.860	0.142	2.055	22	141	63.5	81.5	119
		acetone at 70 K	2.018	2.088	1.859	0.143	2.053	22	141.5	64.5	81.8	119.5
3	$Co(Pmcp)(Bz)^+$	$Fe(cp)(hmBz)PF_6$	2.009	2.079	1.848	0.154	2.044	20	140	65	80	120
4	$Co(Pmcp)(PmBz)^+$	acetone	1.992	2.072	1.900	0.102	2.032	25	131	48	78	106
5	$Co(Pmcp)(hmBz)^+$	$Fe(Pmcp)(hmBz)PF_6$										
		site 1	2.020	2.103	1.912	0.090	2.062	26	140	56	83	114
		site 2	2.001	2.084	1.858	0.144	2.043	20	136	63	78.0	116
		acetone										
		site 1	2.010	2.093	1.876	0.126	2.053	21	140	58	80.5	119
		site 2	1.986	2.067	1.850	0.152	2.027	18	135	65	76.5	117
		acetic anhydride	2.003	2.086	1.860	0.142	2.046	20	141	62	80.5	121
		methylene chloride	2.002	2.085	1.860	0.142	2.045	20	141	62	80.5	121
6	$Co(hmBz)_2^{2+}$	$Fe(hmBz)_2(PF_6)_2$										
		site 1	2.022	2.128	1.858	0.144	2.075	12	137	57	74.5	125
		site 2	2.013	2.119	1.837	0.165	2.066	9	135	59	72	126

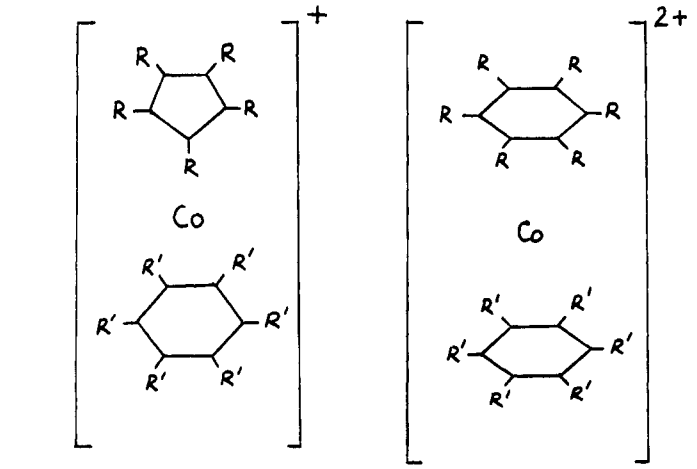

$Co(cp)(Bz)^+$ R=R'=H

$Co(Pmcp)(Bz)^+$ R=CH_3, R'=H

$Co(cp)(hmBz)^+$ R=H, R'=CH_3

$Co(Pmcp)(PmBz)^+$ R=CH_3, all R'=CH_3 except one R'=H

$Co(Pmcp)(hmBz)^+$ R=R'=CH_3

$Co(hmBz)_2^+$ R=R'=CH_3

Figure 1. Structures of the various cobalt (II) mixed-sandwich complexes.

Application of the theory of EPR spectra of d^7 sandwich molecules[8,9] yields the expressions given in Chart I for the spin-Hamiltonian parameters.

In these expressions, $g_e = 2.0023$ is the free electron g value, $k_\parallel$ is the orbital angular momentum reduction factor, V is the vibrational overlap integral frequently called the Ham factor,[10] P and κ are the anisotropic and isotropic hyperfine coupling parameters with P being the free ion value for $g_e\beta_e g_n\beta_n\langle r^{-3}\rangle_{3d}$ and the product $A_F = C_\pi^2P\kappa$ in the Fermi contact term, and x_i and x'_i are coefficients accounting for the mixing of the excited states (obtained on excitation of a σ or δ electron into the π orbital) via spin–orbit coupling ζ. In the static limit, $V = 1$ and $\tan\alpha$ is given by the ratio of the orthorhombic splitting to the effective spin–orbit coupling parameter $(2\delta/\zeta)$. In the dynamic coupling case, which results whenever the static splitting is less than or of the same order of magnitude as one vibrational quantum, only the ratio $\tan\alpha$ and not δ can directly be determined from the spectra. In the strongly distorted situations, exact evaluation of the individual values of $k_\parallel$ and V are not possible. Nevertheless with the aid of MO calculations, the product $k_\parallel V$ related to $\tan\alpha$ by eq 1 can still be made realistic and the values of P, C_π^2, and κ are quite reliable.

Results

Well-resolved EPR spectra were obtained at liquid-helium temperatures for all the compounds studied, in both solid host lattices and frozen solutions. Multiplicity of sites is a common observation in electronically degenerate sandwich compounds because of the extreme sensitivity of the $^2E_{1g}$ and $^2E_{2g}$ ground states to external perturbations caused by the asymmetric lattice potentials. In these cases, the detailed temperature variation of the spectrum was followed up to a point where the more "axial" sites vanish due to faster spin–lattice relaxation, thus leading to simplification of the spectra. The spin-Hamiltonian parameters obtained on simulating this simpler spectrum were carried over as a guide to fit the more complicated lower temperature spectrum. The expected correlation between g_z and $g_\perp$ values as well as the expected constant difference between g_y and g_x values were used for fitting the spectra and assigning the g and A values.

(8) Ammeter, J. H.; Swalen, J. D. *J. Chem. Phys.* **1972**, *57*, 678.
(9) Weber, J.; Goursot, A.; Pénigault, E.; Ammeter, J. H.; Bachmann, J. *J. Am. Chem. Soc.* **1982**, *104*, 1491.
(10) (a) Ham, F. S. *Phys. Rev.* **1965**, *138*, 1727; **1968**, *166*, 307. (b) Sturge, M. D. *Solid State Phys.* **1967**, *20*, 91. (c) Englman, R. *The Jahn-Teller Effect in Molecules and Crystals*; Wiley: New York, 1972.

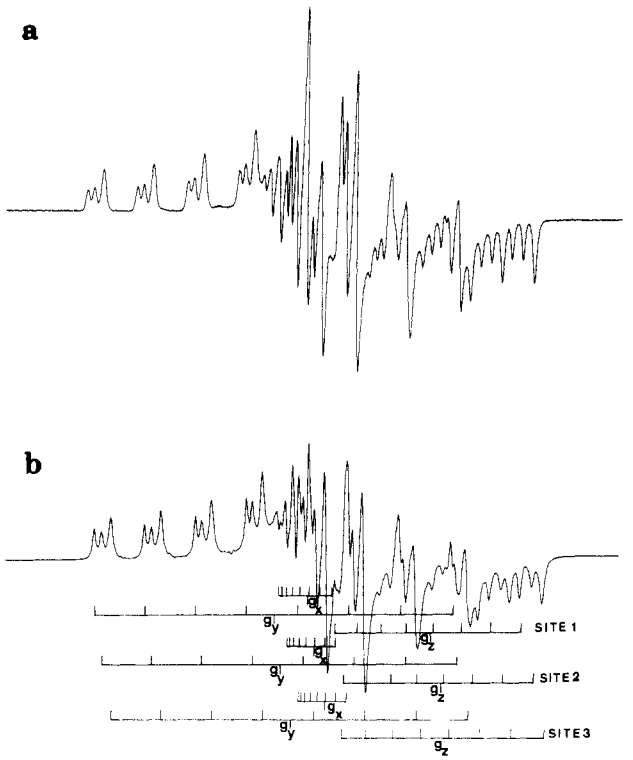

Figure 2. (a) Experimental EPR spectrum of $Co(cp)(Bz)^+$ doped in $Co(cp)_2BF_4$ at 4 K. (b) Spectrum computer simulated with the parameters in Table I.

The EPR parameters for the whole series of cobalt sandwiches studied are collected in Table I. The experimental EPR spectrum of $Co(cp)(Bz)^+$ in a $Co(cp)_2BF_4$ host lattice is shown in Figure 2 along with the computer simulation. Whereas the g_z, A_z and g_y, A_y values are accurate to within ±0.001 for g and ±1.0 × 10^{-4} cm^{-1} for A, the values of g_x and A_x are susceptible to larger errors, viz. ±0.01 for g_x and ±5.0 × 10^{-4} cm^{-1} for A_x, due to the complicated pattern obtained near the center of the spectrum. The assignments of the spin-Hamiltonian g and A components to the molecular framework, z being along the principal molecular axis, was made in analogy with other d^7 sandwich systems studied earlier by us.[2,11]

As the temperature is raised from 4.2 K in all cases the signal initially loses intensity without appreciable broadening. At a certain temperature characteristic of each site in each host lattice, the signal starts broadening and becomes virtually undetectable beyond some higher temperature. We have attempted to fit the temperature-dependent contribution to the line width (W) to an Orbach-type model[12] for spin–lattice relaxation by using

$$W = 1/T_1 = B(\Delta E)^3 e^{-\Delta E/kT} \qquad (3)$$

This variation of line width with temperature was followed in detail for $Co(cp)(Bz)^+$ in $Co(cp)_2BF_4$ where there are three sites, which are separated well enough to follow this variation. Only the y and z components for each site could be followed, and in Figure 3 this variation is shown. An examination of Figure 3 shows that the residual widths in the perpendicular region (y) are greater than that in the parallel (z) region. However the parallel line is found to broaden faster with temperature.

Discussion

The only accurate parameters from the simulation of the EPR spectra are g_y, A_y, g_z, and A_z, with g_x and A_x being not so reliable, and there are seven unknowns in eq 1 and 2: viz. $k_\parallel$, V, tan α, C_π^2, x, x', and κ. Therefore, we have made use of the interrelationships between C_π, $k_\parallel$, and x/x' from the MO model and then have sought a consistent solution by an iterative process.[13] The parameters thus obtained are laid out in Table II. The $k_\parallel$ value for $Co(cp)(Bz)^+$ was evaluated by EHMO calculations using standard procedures.[14] The orbital angular momentum matrix elements over the molecular orbitals were evaluated by using the program written by Rauk and Ichimura.[15] Even though one does not expect $k_\parallel$ to vary appreciably for the same compound in different hosts, there can be substantial effects of methylation on the value of $k_\parallel$. It was found that on going from $Co(cp)_2$ to $Co(Pmcp)_2$ the $k_\parallel$ value reduced from 0.79 to 0.70,[16] which indicates that the effect of methylation is to increase covalency. For an initial analysis, however, we assumed that the same value of $k_\parallel$ can be used through out the mixed-sandwich series, and this led to clear separation of the unmethylated and fully methylated compounds in all the correlation plots for, e.g., $\delta(g_z)$ vs. $g_\perp$ (Figure

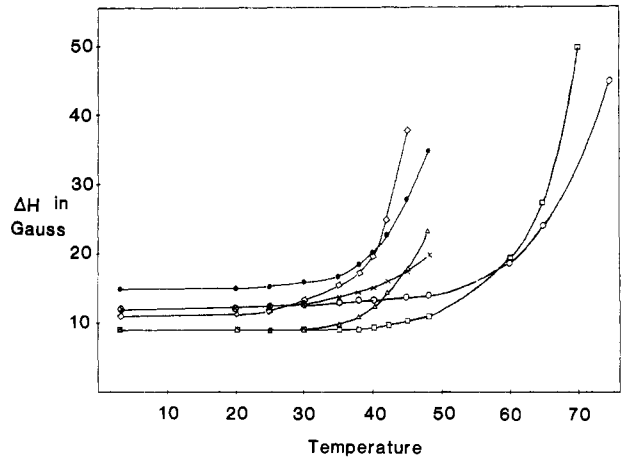

Figure 3. Temperature dependence of line width for the three sites of $Co(cp)(Bz)^+$ doped in $Co(cp)_2BF_4$. The nomenclature of the sites as in Table I. Key: (○) site 1, y component; (□) site 1, z component; (×) site 2, y component; (△) site 2, z component; (●) site 3, y component; (◇) site 3, z component.

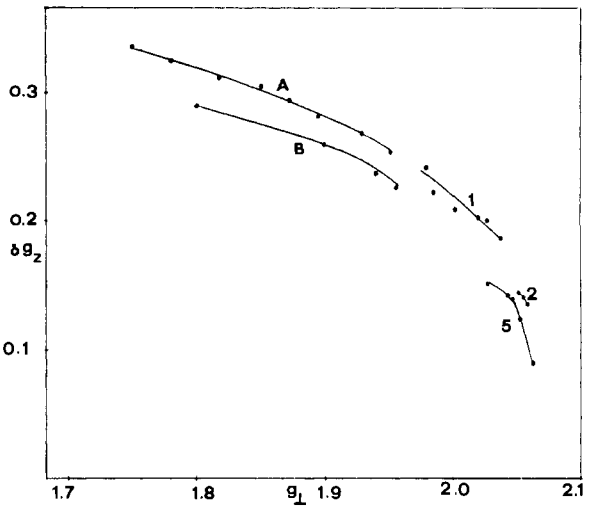

Figure 4. Correlation of $\delta(g_z)$ and $g_\perp$ for the cobalt(II) mixed sandwiches, with the numbers referring to Table I. The points corresponding to cobaltocenes (A) and to iron(I) mixed sandwiches (B) are also shown for the sake of comparison.

(11) Rajasekharan, M. V.; Giezynski, S.; Ammeter, J. H.; Oswald, N.; Michaud, P.; Hamon, J. R.; Astruc. D. *J. Am. Chem. Soc.* **1982**, *104*, 2400.
(12) Orbach, R.; Stapleton, J. H. In *Electron Paramagnetic Resonance*; Geschwind, S., Ed.; Plenum: New York, 1972; pp 121–216.
(13) Rajasekharan, M. V.; Bucher, R.; Deiss, E.; Zoller, L.; Salzer, A. K.; Weber, J.; Ammeter, J. H., submitted for publication.
(14) (a) Ballhausen, C. J.; Gray, H. B. *Molecular Orbital Theory*; Benjamin: New York, 1964. (b) Ammeter, J. H.; Bürgi, H. B.; Thiebeault, J. C.; Hoffmann, R. *J. Am. Chem. Soc.* **1978**, *100*, 3686.
(15) Ichimura, H.; Rauk, A. *J. Chem. Phys.* **1973**, *59*, 5720.
(16) Zoller, L. Ph.D. Thesis, University of Zurich, Anorganische Chemie Institut, 1983.

Table II. Jahn–Teller and Bonding Parameters Derived for Co(II) Sandwich Compounds

no.	compd	matrix	$k_\parallel$	V	$k_\parallel V$	tan α	P^a	C_π^2	κ	10^2x	x/x'
1	$Co(cp)(Bz)^+$	$Co(cp)_2BF_4$									
		site 1	0.817	1.0	0.817	10.7	148.3	0.58	71.6	0.88	2.02
		site 2	0.816	0.894	0.729	7.17	147.3	0.58	70.0	0.88	2.04
		site 3	0.810	0.670	0.543	5.15	145.2	0.56	72.6	0.88	2.11
		$Co(cp)_2PF_6$									
		site 1	0.820	0.58	0.476	4.30	145.0	0.57	72.4	0.87	2.14
		site 2	0.812	0.53	0.429	3.99	144.0	0.56	72.6	0.87	2.15
		$Fe(cpXBz)PF_6$	0.817	0.842	0.688	6.82	147.1	0.58	71.5	0.87	2.10
		acetic anhydride	0.820	0.867	0.711	7.00	149.2	0.59	72.8	0.88	2.07
		methylene chloride	0.819	0.912	0.747	7.90	148.3	0.58	71.2	0.87	2.04
2	$Co(cp)(hmBz)^+$	$Fe(cpXhmBz)PF_6$	0.780	1.0	0.780	18.2	142.2	0.56	76.5	1.07	2.15
		acetic anhydride	0.770	0.98	0.755	16.0	139.8	0.55	76.2	1.07	2.14
		acetone	0.775	0.89	0.690	13.0	142.2	0.56	75.2	1.07	2.15
3	$Co(Pmcp)(Bz)^+$	$Fe(cp)(hmBz)PF_6$	0.75	0.69	0.517	6.9	137.0	0.54	78.8	1.12	2.07
4	$Co(Pmcp)(PmBz)^+$	acetone	0.72	0.52	0.38	5.5	132.0	0.52	80.0	1.20	2.02
5	$Co(Pmcp)(hmBz)^+$	$Fe(PmcpXhmBz)PF_6$									
		site 1	0.71	1.0	0.71	18.8	132	0.52	82	1.31	2.09
		site 2	0.70	0.728	0.51	7.0	133.5	0.525	81.8	1.28	2.05
		acetone									
		site 1	0.71	0.929	0.66	9.7	134.6	0.53	82.1	1.29	2.04
		site 2	0.71	0.53	0.38	5.0	131.0	0.515	82.5	1.27	1.99
		acetic anhydride	0.72	0.722	0.52	7.3	132	0.52	83	1.28	2.01
		methylene chloride	0.70	0.728	0.51	7.1	131.0	0.51	82.2	1.28	2.05
6	$Co(hmBz)_2^{2+}$	$Fe(hmBz)_2(PF_6)_2$									
		site 1	0.80	1.0	0.80	11.8	148	0.58	73.8	1.61	1.71
		site 2	0.80	0.825	0.66	7.9	145	0.56	75.0	1.59	1.73

[a] P in 10^{-4} cm^{-1}.

4), V vs. tan α, etc. Moreover, the data analysis of the EPR parameters yielded a slightly larger value of C_π^2 for Co(Pmcp)(hmBz)$^+$ as opposed to Co(cp)(Bz)$^+$ (0.62 for Co(Pmcp)(hmBz)$^+$ and 0.58 for Co(cp)(Bz)$^+$), which is contrary to what one would have expected on the basis of the guideline, increased covalency on methylation. Hence we carried out EHMO and angular momentum calculations on the various methylated derivatives to evaluate $k_\parallel$ for each case. We have found a larger reduction of $k_\parallel$ on the methylation of the cyclopentadienyl ring than on the methylation of the benzene ring, and for the fully methylated Co(Pmcp)(hmBz)$^+$, the $k_\parallel$ value is reduced by 15% from 0.82 to 0.70. These are in general agreement with the usual chemical arguments and also earlier electrochemical and NMR experimental results on these compounds.[4] A more detailed analysis[16] of these calculations reveals that the large reduction of $k_\parallel$ upon methylation is only to a small degree due to a covalency increase; the largest effect comes from the ligand orbital part of the total angular momentum, $\gamma_\parallel$. The parameters in Table II are based on these differences in $k_\parallel$ as obtained from molecular orbital calculations. We see from Figure 4 where the data of $Co(cp)_2$ are also plotted, that the $\delta(g_z)$ vs. $g_\perp$ correlation for Co(cp)(Bz)$^+$, follows closely that of $Co(cp)_2$ with the points corresponding to situations with larger distortions. In a way it is almost a continuation of the $Co(cp)_2$ curve toward the static limit. On the other hand, the points corresponding to the methylated compounds lie further toward the static limit and do not follow the extrapolated variation of Co(cp)(Bz)$^+$. The comparison with Fe(cp)(Bz), whose data points are also shown in Figure 4, reveals that the cobalt mixed-sandwich systems are more covalent (i.e. show larger delocalization of spin density on the ligand rings) than the iron analogues.

From the value of $k_\parallel V$ obtained from the analysis of the EPR parameters, we can get out the value of V through the use of the $k_\parallel$ values from molecular orbital calculations. The plot of V vs. tan α is shown in Figure 5, and a comparison of $Co(cp)_2$ alkylated cobaltocenes and the mixed-sandwich systems is made. It is seen that, even on the basis of smaller $k_\parallel$ values for Co(Pmcp)(hmBz)$^+$, not all the points fall on a continuous smooth curve. A reduction in $k_\parallel$ is seen, and a similar conclusion has been drawn for the case of $Ni(cp)_2^+$ and its methylated analogues.[17] It is also evident

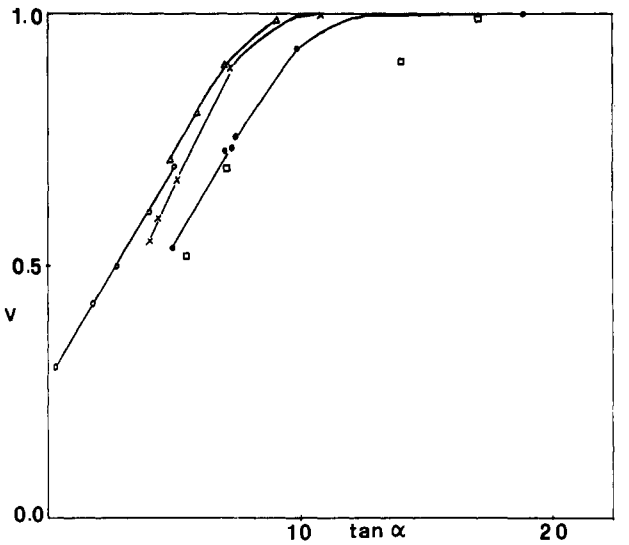

Figure 5. Plot of V vs. tan α for the cobalt(II) mixed sandwiches. Cobaltocene (○) and alkylated cobaltocenes (△) are also shown in the graph. –×–×– refers to Co(cp)(Bz)$^+$ and –●–●– to Co(Pmcp)(hmBz)$^+$. □ points refer to the other methylated derivatives.

from this figure that vibronic coupling effects on the ground-state properties are significant as long as the orthorhombic field is below about 3000 cm^{-1} (obtained from tan $\alpha = 2\delta/\zeta$ with $\zeta = 350$ cm^{-1}), i.e. ca. four quanta of the active vibrational mode. This seems to be a general conclusion for most of the metallocenes studied so far, and the small differences observed could be due to the differences in spin–orbit coupling of the frequencies of the active modes etc. The apparent differences may not even be significant in view of the uncertainties of $k_\parallel$, C_π^2, ζ, and tan α. The C_π^2 values derived from the analysis of the spin-Hamiltonian parameters for the mixed-sandwich systems are consistently less than those determined for either cobaltocene or Fe(I) mixed-sandwich compounds with less than 60% of the electron density on the metal. However, the values for $Ni(cp)_2^+$ are less than those of the cobalt mixed-sandwich compounds. The highest occupied molecular orbital of Co(cp)(Bz)$^+$ and its methylated derivatives is therefore more delocalized than in $Co(cp)_2$ and Fe(cp)(Bz) but less delocalized than in $Ni(cp)_2^+$.

(17) Moser, E. Diploma Thesis, University of Zurich, Anorganische Chemie Institut, 1983.

Table III. Analysis[a] of V as a Function of $\delta(g)$ and x_σ/x_δ for Co(Pmcp)(hmBz)$^+$ in the Most Distorted Situation

	$\delta(g)$						
x_σ/x_δ	0.080	0.081	0.082	0.083	0.084	0.085	0.086
1.0	>1	0.93	0.80	0.72	0.65	0.60	0.57
1.05	>1	>1	0.92	0.80	0.72	0.66	0.63
1.10	>1	>1	1.001	0.92	0.79	0.72	0.69
1.15	>1	>1	>1	1.00	0.88	0.78	0.76
1.20	>1	>1	>1	>1	0.997	0.88	0.83
1.25	>1	>1	>1	>1	>1	0.96	0.90
1.30	>1	>1	>1	>1	>1	>1	0.997

[a] Taking $k_\parallel$ from EHMO calculations to be 0.71 and thus $V(\cos\alpha)$ $(=\Delta g_z/2k_\parallel)$ to be 0.0556 for the case of Co(Pmcp,hmBz)$^+$ in Fe(Pmcp,hmBz)PF_6, site 1.

The x values, which are inversely related to the average $\sigma \rightarrow \pi$ and $\delta \rightarrow \pi$ transition energies and directly to the value of $k_\perp$ (determined by the covalency of the z^2, xy, and $x^2 - y^2$ orbitals), are larger in the cobalt mixed sandwiches than in the corresponding Fe(I) sandwiches. Larger covalency and smaller average energy separations do not seem compatible, and hence a more detailed analysis is warranted. We feel that for the more distorted situations the average energy approximation is not quite good enough, and consideration of the individual ΔE's is necessary. This leads to two values of x and the corresponding equations for the **g** tensor now read as

$$g_\perp = (g_e + 2x_\delta + 3x_\sigma)(\sin\alpha) \quad (4a)$$

$$\delta(g) = 6(1 + V(\cos\alpha))x_\sigma \quad (4b)$$

As we need the value of V for this analysis, we have chosen the most distorted site of Co(Pmcp)(hmBz)$^+$ for the illustration where we believe that the static limit has been reached and hence V can be taken to be 1.0. Assuming different values of $\delta(g)$ (as g_x cannot be determined accurately from the spectral simulation and this uncertainty is one of the hurdles in the accurate determination of the bonding and Jahn–Teller parameters), the corresponding value of x_σ is evaluated. For each x_σ, $\sin\alpha$ is calculated as a function of the ratio x_σ/x_δ and thus V is evaluated as a function of $\delta(g)$ and x_σ/x_δ (shown in Table III). We note that approximately along the diagonal V attains the value of 1.0, and we can now choose among the various possible combinations of $\delta(g)$ and x_σ/x_δ all of which yield the value of V to be unity. From EHMO calculations on Co(Pmcp)(hmBz)$^+$,[18] we have found that the value of the ratio $\Delta E_{\delta\rightarrow\pi}/\Delta E_{\sigma\rightarrow\delta}$ is 1.150. As x is inversely proportional to ΔE, the ratio of x_σ/x_δ can also be taken to be 1.150. The value of g_x corresponding to the above ratio is what is reported in Table I, and we have used this value of g_x in further analysis. The bonding parameter, C_π^2, however, has been found to be quite insensitive to the value of the ratio x_σ/x_δ for a given value of $\delta(g)$.

From line width dependence on temperature a value of ΔE (eq 3) has been obtained, assuming an Orbach type process for relaxation. For Co(cp)(Bz)$^+$ doped in $Co(cp)_2BF_4$ where there are three sites, two different ΔE's are obtained for the z and y components of each site. The values are laid out in Table IV. The residual line widths at low temperatures originate mainly in a random distribution of the rhombic distortion δ, which causes a spread in the g values. Thus qualitatively one can explain the fact that the residual widths in the y component are greater than that in the z component on the basis of the $\delta(g_z)$ vs. $g_\perp$ plot. As the temperature is raised, lifetime broadening via spin–lattice relaxation becomes significant. The reasonably good quality of the exponential fit obtained is an indication that direct and Raman processes make less important contributions to the spin–lattice relaxation, but at present our accuracy of temperature measurement and inability to separate relaxation effects and inhomogeneous broadening contributions make more detailed analysis difficult. The coefficient B in all cases turn out to be in the range of 10^{-4}, which is several orders of magnitude smaller than the typical values observed for the Orbach process in ionic lattices, and this indicates a rather weak coupling of the spin system with the phonons of the lattice. The ΔE's obtained are rather small compared to δ, and this suggests that a linear single-mode approximation used here may not be quite adequate or that Raman (T^7) and direct (T^2) processes are not making negligible contributions as we have assumed.

Table IV. Residual Line Widths at Low Temperatures, Orbach Parameters, and Rhombic Splitting Parameters for the Sites of Co(cp)(Bz)$^+$ in $Co(cp)_2BF_4$

	residual line width, G	B	ΔE, cm^{-1}	$2\delta_0$,[a] cm^{-1}
site 1				
y	12.0	5.5×10^{-5}	293	2002
z	9.0	1.8×10^{-4}	405	
site 2				
y	12.0	8.6×10^{-5}	250	1348
z	9.0	2.2×10^{-4}	380	
site 3				
y	15.0	1.4×10^{-4}	214	968
z	11.4	3.1×10^{-4}	340	

[a] $2\delta_0 = C_\pi^2\zeta(\tan\alpha)$ with $\zeta = 330$ cm^{-1}.

Summary and Conclusions

Cobalt (II) mixed-sandwich complexes with different degrees of ligand substitution ranging from the unsubstituted Co(cp)(Bz)$^+$ to the fully methylated Co(Pmcp)(hmBz)$^+$ have been investigated by EPR. The results are in agreement with the expected d^7 $^2\pi$ ground state with the unpaired electron in the e_{1g} orbital having mainly metal ($d_{xz}d_{yz}$) character. There is clear evidence for a dynamic Jahn–Teller effect from the characteristic host lattice dependence of EPR parameters; varying ligand substitution and host lattice, we have been able to cover examples from the dynamic to the static case. Methyl substitution increases covalency as seen by comparing Co(cp)(Bz)$^+$ with Co(Pmcp)(hmBz)$^+$ with the methylation of the cyclopentadienyl ring having a larger effect than the methylation of the benzene ring. Consistently lower values of C_π^2 have been obtained for these mixed sandwiches as compared to cobaltocenes and Fe(I) mixed-sandwich compounds. The C_π^2 values of Ni(III) sandwich compounds are lower than for the Co(II) mixed sandwiches. We have not been able to obtain highly "axial" sites in any host lattice even for the unsubstituted Co(cp)(Bz)$^+$, and the lowest tan α value so far in the mixed cobalt sandwiches is 3.99. The temperature dependence of line width in Co(cp)(Bz)$^+$ doped in $Co(cp)_2BF_4$ could be fit to an Orbach type equation, but the ΔE's obtained are much lower than the value of the orthorhombic distortion δ. However, more direct measurement of ΔE, for example by using the inelastic neutron scattering method, as well as more detailed calculations using the multimode coupling case would be necessary in settling the questions of the relaxation mechanisms.

Registry No. **1**, 90246-06-3; **2**, 90246-02-9; **3**, 90246-00-7; **4**, 90245-96-8; **5**, 90246-11-0; **6**, 53382-66-4; $Co(cp)_2BF_4$, 52314-53-1; Fe(cp)(Bz)PF_6, 12176-31-7; Fe(cp)(hmBz)PF_6, 53702-66-2; Fe(Pmcp)(hmBz)PF_6, 71713-57-0; $Fe(hmBz)_2(PF_6)_2$, 53382-63-1.

(18) In all the mixed-sandwich systems a standard metal–ring distance was used; viz., metal–benzene ring distance = 1.6 Å, and metal–cyclopentadienyl ring distance = 1.8 Å. This need not be constant throughout the series and probably leads to erroneous comparisons, but the lack of any crystal structural data on these compounds forces us to make the assumption.